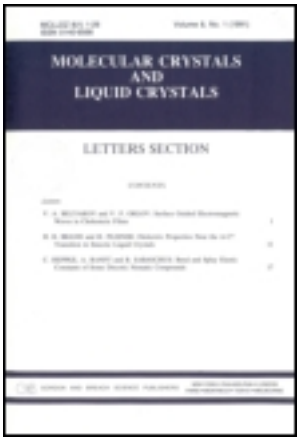

Molecular Crystals and Liquid Crystals
Publication details, including instructions for authors and subscription information:
http://www.tandfonline.com/loi/gmcl20

Novel Ruthenium Complex with Terpyridine Derivative for DSSCs

Dong Min Chang [a] , Dong Yuel Kwon [b] & Young Sik Kim [a c]
[a] Department of Information Display , Hongik University , Seoul , 121-791 , Korea
[b] Department of chemical engineering , Hongik University , Seoul , 121-791 , Korea
[c] Department of Science , Hongik University , Seoul , 121-791 , Korea
Published online: 08 Jan 2014.

To cite this article: Dong Min Chang , Dong Yuel Kwon & Young Sik Kim (2013) Novel Ruthenium Complex with Terpyridine Derivative for DSSCs, Molecular Crystals and Liquid Crystals, 585:1, 91-99, DOI: 10.1080/15421406.2013.849524

To link to this article: http://dx.doi.org/10.1080/15421406.2013.849524

Mol. Cryst. Liq. Cryst., Vol. 585: pp. 91–99, 2013

ISSN: 1542-1406 print/1563-5287 online
DOI: 10.1080/15421406.2013.849524

Taylor & Francis
Taylor & Francis Group

Novel Ruthenium Complex with Terpyridine Derivative for DSSCs

DONG MIN CHANG,[1] DONG YUEL KWON,[2] AND YOUNG SIK KIM[1,3,*]

[1]Department of Information Display, Hongik University, Seoul 121-791, Korea
[2]Department of chemical engineering, Hongik University, Seoul 121-791, Korea
[3]Department of Science, Hongik University, Seoul 121-791, Korea

In this work, we designed and investigated theoretically novel ruthenium(II) complex (Bu_4N)[Ru(DMFAdctpy)$(NCS)_3$]; (DMFAdctpy : 2-(6-(5-(4-(bis(9,9-dimethyl-9H-fluoren-2-yl)amino)phenyl)pyridin-2-yl)-4-carboxypyridin-2-yl)pyridine-4-carboxylic acid) with DMFAdctpy as an anchoring group and a highly conjugated ancillary ligand to increase absorption ability in the long wavelength region compared to the N3 dye([Ru(dcbpy)$_2$$(NCS)_2$]); (dcbpy (4,4′-dicarboxy-2,2′-bipyridine)). The density functional theory (DFT) and time-dependent density functional theory (TD-DFT) calculations were used to gain insight into the factors responsible for photovoltaic properties as dye sensitizer. The absorption spectrum of these dyes with terpyridine derivative is more red-shifted and broad than that of N3, especially, in the region between 400 nm and 650 nm. This is attributed to the extension of the π-conjugated system of insertion terpyridine ligands. Molecular orbital analysis confirmed that the HOMOs of (Bu_4N)[Ru(DMFAdctpy)$(NCS)_3$] localized over the NCS ligand orbitals. The LUMO, LUMO+1 and LUMO+2 are mainly localized over the dctpy ligand. However, the LUMO+3 is delocalized on the DMFA moiety. Due to the panchromatic and red-shifted absorption spectrum, these novel ruthenium complexes are expected to good candidates as dye sensitizers for DSSCs.

Keywords Dye-sensitized solar cells (DSSCs); Ruthenium; terpyridine; TD-DFT; DFT

Introduction

Recently much attention has been focused on the dye-sensitized solar cells (DSSCs), as possible low-cost photovoltaic devices [1]. Performance and stability of DSSC devices have been studied and significantly developed over the past decade [2–4]. Among the components of DSSC, the sensitizer is a crucial element, which significantly influences on the power conversion efficiency as well as the stability of the device. Up to now, the record for DSSC efficiency was held by a polypyridyl ruthenium sensitizer (11%) in combination with a voltaic iodide/triiodide mixture as electrolyte [5]. However, the conversion efficiency of DSSCs is still lower than that of the silicon-based photovoltaic cells. To obtain a high conversion efficiency, optimization of the short-circuit photocurrent (Jsc) and open-circuit potential (Voc) of the cell is essential. The value of Voc depends on the edge of conduction

*Address correspondence to Prof. Young Sik Kim. Tel: (+82) 2-320-1607, Fax: (+82) 2-3142-0335. E-mail: youngkim@hongik.ac.kr

band in TiO_2 and the redox potential of I-/ I3-, otherwise Jsc is related to the interaction between TiO_2 and the sensitizer as well as the absorption coefficient of the sensitizer [6]. Furthermore, Jsc is closely related to the metal-to-ligand charge transfer (MLCT) transition of immobilized dye molecules, which could be improved significantly by means of the enrichment electron-donating ability of the ancillary ligand [7].

In order to enhance power conversion efficiencies of DSSCs, it is imperative to design novel sensitizers that exhibit an enhanced molar extinction coefficient in combination with a red-shifted absorption band compared to standard $[Ru(dcbpy)_2(NCS)_2]$ (N3). Extension of the π-conjugation of the ancillary ligand and/or the anchoring ligand can improve the spectral response of corresponding ruthenium sensitizers [8]. Therefore, efforts were recently made to increase the molar extinction coefficients of the ruthenium dyes in order to improve their light-harvesting ability. In this work, we designed a novel ruthenium complex $(Bu_4N)[Ru(DMFAdctpy)(NCS)_3]$ with high π-conjugated DMFAdctpy group. The density functional theory (DFT) and time-dependent density functional theory (TD-DFT) calculations were used to estimate the photovoltaic properties of the dyes [9]. Finally, we will suggest high performed dye sensitizer as a DSSC device.

Computational Methods

To gain insight into the factors responsible for the absorption spectral response and the conversion efficiency, we perform DFT and TD-DFT calculations on the ground state of the ruthenium dyes. This computational procedure allows us to provide a detailed assignment of the excited states involved in the absorption process. The geometries and energy levels of molecular orbital were calculated by the DFT method and the absorption spectrum was calculated at optimized ground state geometries by the TD-DFT method. Although, the energy levels of molecular orbital can predict the trend of energy gap in the absorption spectrum, their data do not exactly match in the absorption spectrum. Since the absorption process has time dependency, the absorption spectrum in this study originates from TD-DFT.

The geometries in the gas phase were optimized by the DFT method using the B3LYP/DGDZVP in the Gaussian 03 program package. The HOMO is the highest occupied molecular orbital, HOMO-1 is the next highest occupied molecular orbital, and HOMO-2 is the second highest occupied molecular orbital. The LUMO is the lowest unoccupied molecular orbital, LUMO-1 is the next lowest unoccupied molecular orbital, and LUMO-2 is the second lowest unoccupied molecular orbital. Electronic populations of HOMO and LUMO were calculated to show the position of the localization of electron populations along with the calculated molecular orbital energy diagram.

TD-DFT calculations with B3LYP/DGDZVP level of theory were performed at the ground state optimized geometries by means of the C-PCM algorithm, as implemented in the G03 program package. Absorption spectrum was calculated at optimized ground state geometries for lowest 30 singlet-singlet excitations up to wavelength of 400 nm. The simulation of the absorption spectra was performed by a Gaussian convolution with fwhm = 0.27 eV.

Results and Discussion

The chemical structures of dyes studied herein are shown in Figure 1. The $(Bu_4N)[Ru(DMFAdctpy)(NCS)_3]$ was designed by adding the DMFA on the dctpy moiety.

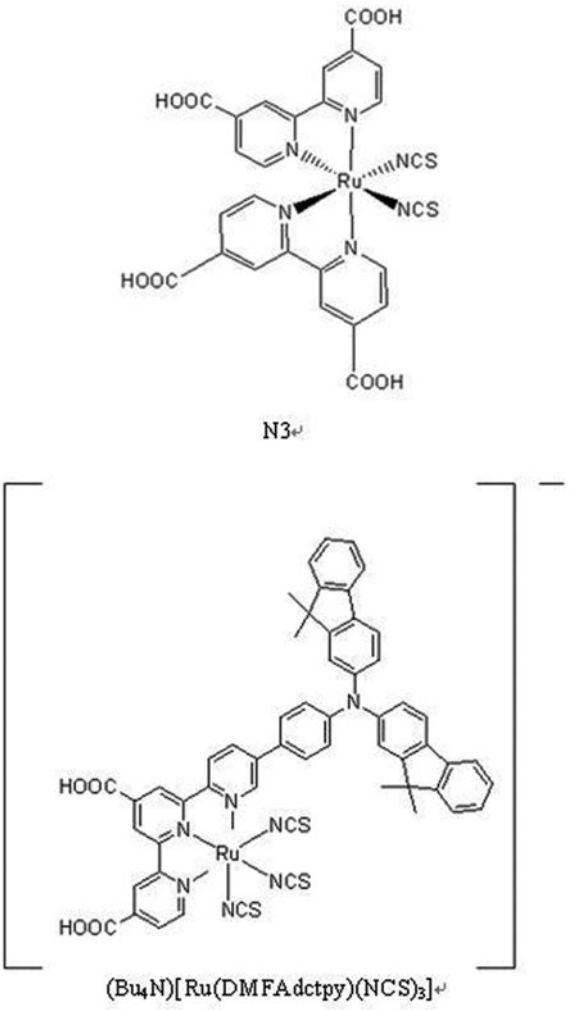

Figure 1. Molecular structure of the dyes : N3 and $(Bu_4N)[Ru(DMFAdctpy)(NCS)_3]$.

To increase the power conversion efficiency, the DMFAdctpy ligand was designed for extension of the π-conjugation system and enrichment the electron-donating ability. The π-conjugation system and enrichment the electron-donating ability would lead to red-shifted, broadened absorption band and improve the MLCT [6–8]. Therefore, the $(Bu_4N)[Ru(DMFAdctpy)(NCS)_3]$ is expected to better performance in Jsc than the N3. DFT calculations were performed at a B3LYP/DGDZVP level for the geometry optimization of these dyes in order to obtain molecular orbitals and electronic structures of the N3 and the $(Bu_4N)[Ru(DMFAdctpy)(NCS)_3]$.

These dyes with their isodensity surface plots of the frontier MOs (Molecular Orbitals) are shown in Figure 2. It shows that the HOMO orbitals of the N3 and (Bu_4N) $[Ru(DMFAdctpy)(NCS)_3]$ are localized over the NCS groups, respectively. In the case of the N3, LUMO orbitals are mainly localized on the dcbpy groups. Whereas, in the case of $(Bu_4N)[Ru(DMFAdctpy)(NCS)_3]$, the LUMO is localized over the dctpy and NCS groups.

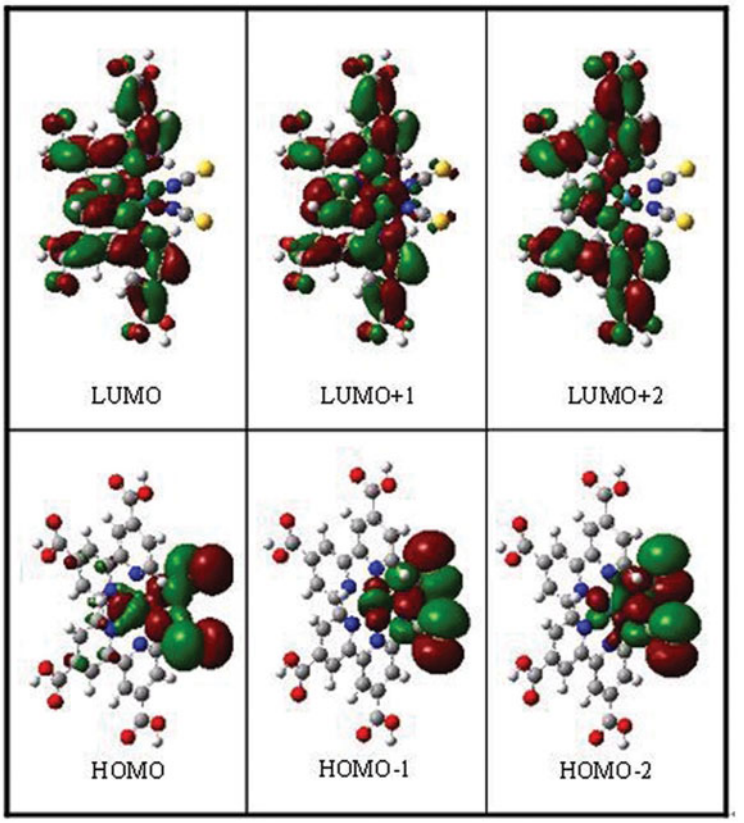

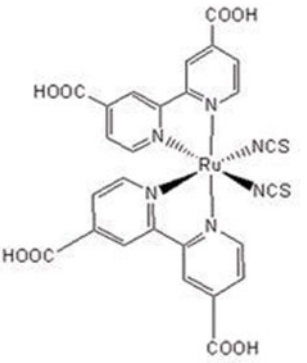

N3

Figure 2. Frontier molecular orbitals (HOMOs, LUMOs) : (a) N3 (b) $(Bu_4N)[Ru(DMFAdctpy)(NCS)_3]$. *(Continued)*

Furthermore, the LUMO+1 and the LUMO+2 are mainly delocalized on the dctpy moiety and the LUMO+3 is mainly delocalized on the DMFA.

Figure 3 shows the calculated molecular orbital energy diagram for these dyes. HOMO and LUMO are acronyms for highest occupied molecular orbital and lowest unoccupied

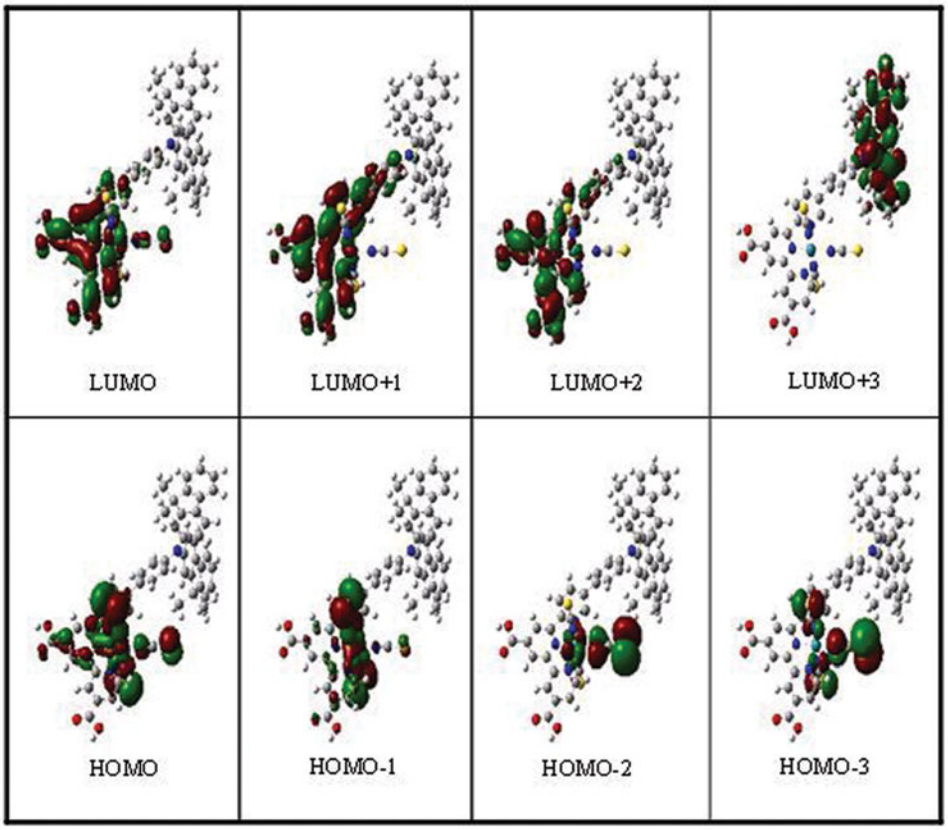

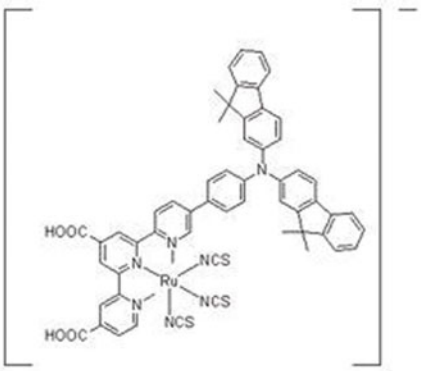

$(Bu_4N)[Ru(DMFAdctpy)(NCS)_3]$

Figure 2. (Continued)

molecular orbital, respectively. The difference of the energies of the HOMO and LUMO, termed the band gap can sometimes serve as a measure of the excitability of the molecule; the smaller the energy the more easily it will be excited. The HOMO level is to organic semiconductors what the valance band is to inorganic semiconductors. The same analogy

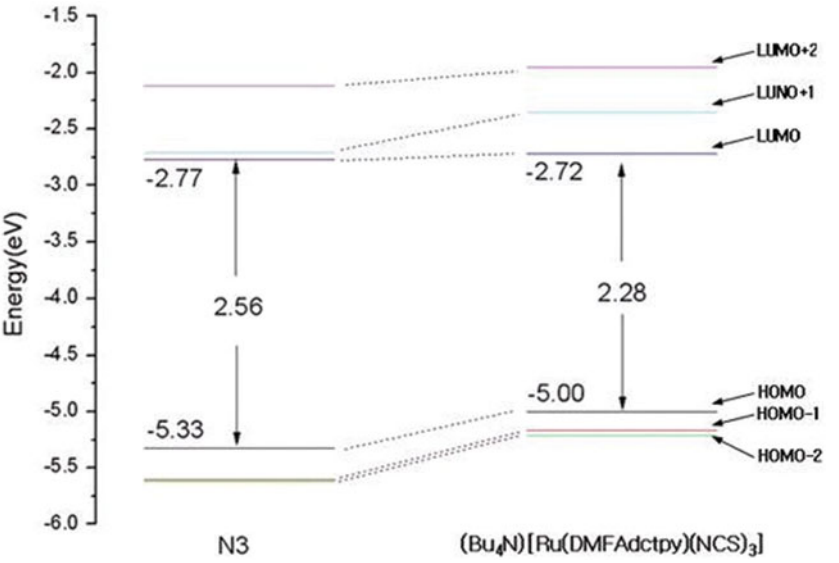

Figure 3. Schematic energy diagram for N3 and $(Bu_4N)[Ru(DMFAdctpy)(NCS)_3]$.

excites between the LUMO level and the conduction band. The energy difference between the HOMO and LUMO level is regarded as band gap energy. When the molecule forms a dimmer or an aggregated, the proximity of the orbital of the different molecules induce a splitting of the HOMO and LUMO energy levels. This splitting produces vibrational sublevels as there are molecules that interact together. When there are enough molecules influencing each other (e.g. in an aggregate), there are so many sublevels that we no longer perceive their discrete nature; they form a continuum.

Overall, energy gaps between HOMOs and LUMOs levels of the $(Bu_4N)[Ru(DMFAdctpy)(NCS)_3]$ were decreased with additional DMFAdctpy group. Specifically, HOMOs levels of the $(Bu_4N)[Ru(DMFAdctpy)(NCS)_3]$ were destabilized by the electron-donating characteristic of DMFAdctpy group. These results lead to the reduction of energy gaps between HOMOs and LUMOs levels when compared with that of the N3. The reduction of the energy gap of the dye would show more red-shifted band in the absorption spectrum and panchromatic absorption band in the long wavelength region.

Figure 4 shows the UV-Vis absorption spectra of the N3 and the $(Bu_4N)[Ru(DMFAdctpy)(NCS)_3]$ by TDDFT calculations. The red-shifted absorption band in all around visible light region of $(Bu_4N)[Ru(DMFAdctpy)(NCS)_3]$ is in agreement with the extension of π-conjugation of the DMFAdctpy moiety, which results in decrease between HOMOs and LUMOs levels than that of the N3. The absorption peaks at 368 nm, 428 nm, 554 nm and 668 nm of the N3 are mainly contributed from HOMO-5 $\rightarrow$ LUMO, HOMO-2 $\rightarrow$ LUMO+2, HOMO-2 $\rightarrow$ LUMO and HOMO $\rightarrow$ LUMO transition, respectively (see Table 1). The absorption peaks at 364 nm, 454 nm, 522 nm and 585 nm of $(Bu_4N)[Ru(DMFAdctpy)(NCS)_3]$ are mainly contributed from HOMO-1 $\rightarrow$ LUMO+3, HOMO-2 $\rightarrow$ LUMO+2, HOMO $\rightarrow$ LUMO+1 and HOMO $\rightarrow$ LUMO transition, respectively. Especially, the absorption peak at 364 nm is remarkably higher than that of N3, which peak is originated from the HOMO-1 $\rightarrow$ LUMO+3 (46%) transition. Focused on the absorption band at 454 nm and 522 nm of $(Bu_4N)[Ru(DMFAdctpy)(NCS)_3]$, these peaks

Table 1. Calculated TDDFT excitation energies (eV, nm), oscillator strengths (f) and composition in terms of MO contributions: N3 and [Ru(DMFAtpy)(dctpy)]

Dye	# of excited state	Calculated energy(eV, nm)	Oscillator strength(f)	Major composition
N3	1	3.3099(374.59)	0.0747	H-5->LUMO (83%)
	2	2.9841(424.0)	0.0794	H-2->L+2 (58%)
	3	2.2302(555.94)	0.1379	H-2->LUMO (51%), H-1->L+1 (39%)
	4	1.8464(671.5)	0.0346	HOMO->LUMO (91%)
[Ru(DMFAtpy)(dctpy)]	1	3.265(379.73)	0.1299	H-1->L+3 (46%), HOMO->L+3 (26%)
	2	2.7125(457.08)	0.0946	H-2->L+2 (85%)
	3	2.3963(517.41)	0.2004	HOMO->L+1 (72%), H-1->L+1 (17%)
	4	2.0476(605.5)	0.1143	HOMO->LUMO (75%), H-1->LUMO (16%)

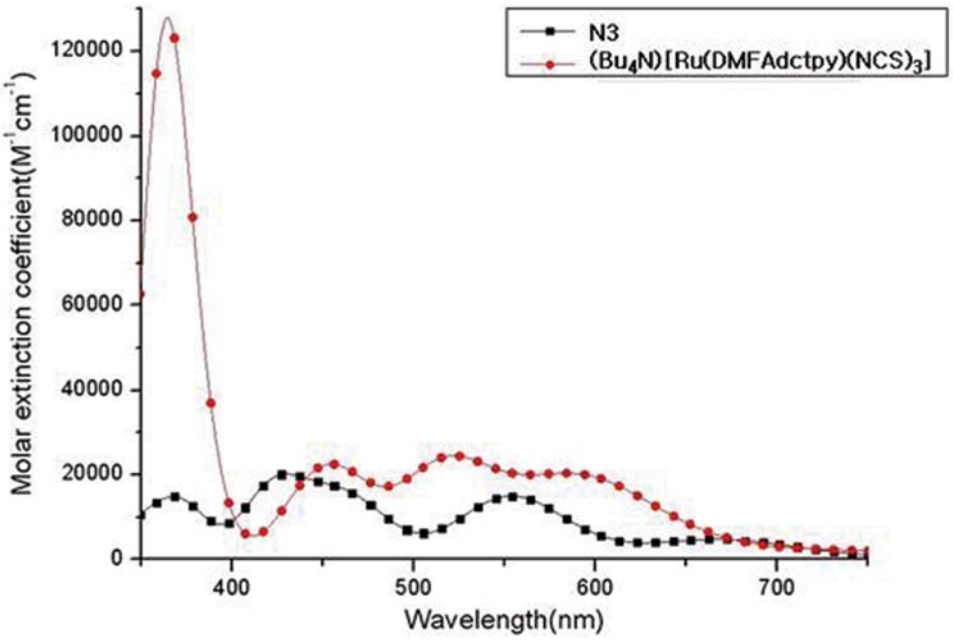

Figure 4. The calculated absorption spectra of the dyes: N3 and $(Bu_4N)[Ru(DMFAdctpy)(NCS)_3]$.

are originated from the HOMO-2 → LUMO+2 (85%) and HOMO → LUMO+1 (72%) transitions, respectively. As shown in Fig. 2 and Fig. 3, the LUMO+1 and LUMO+2 were localized over the dctpy moiety and the LUMO+3 was localized on the DMFAdctpy moiety. Moreover, HOMOs levels were destabilized by introducing DMFAdctpy ligand. Therefore, the significantly increase of the molar extinction coefficients at 368 nm and the red-shifted absorption band around 400 nm to 650 nm are due to the introduction of DMFAdctpy as an ancillary ligand. Furthermore, absorption energy bands of $(Bu_4N)[Ru(DMFAdctpy)(NCS)_3]$ showed enhanced molar extinction coefficients between 400 nm and 650 nm in the visible light region, compared with N3, due to the π-conjugated DMFAdctpy group as a weak donor. These results, reveals that the presence of the DMFAdctpy ligand can reinforce the electron-donating ability of the ancillary ligand thereby may also be able to enhance the spectral response of the corresponding ruthenium sensitizer. Therefore, the $(Bu_4N)[Ru(DMFAdctpy)(NCS)_3]$ would be expected high light-harvesting and conversion efficiency as a photovoltaic device.

Conclusions

Novel ruthenium complex with DMFAdctpy ligand was designed and studied theoretically for the potential devices of DSSCs. Specifically, structural, electronic and optical properties of the $(Bu_4N)[Ru(DMFAdctpy)(NCS)_3]$ were investigated with the introduction to DMFAdctpy as an ancillary ligand. In electronically, HOMOs levels were destabilized by the electron-donating characteristic of DMFAdctpy. The absorption spectra of the $(Bu_4N)[Ru(DMFAdctpy)(NCS)_3]$ showed more broad and red-shifted by the additional DMFAdctpy ligand. Moreover, the molar extinction coefficients significantly increase at 364 nm and between 400 nm and 650 nm. This means that the DMFAdctpy ligand can reinforce the electron-donating ability of the ancillary ligand thereby may also be able to enhance the spectral response of the corresponding ruthenium sensitizer. Therefore, $(Bu_4N)[Ru(DMFAdctpy)(NCS)_3]$ is expected to efficient light harvesting and better performance in J_{sc} than the N3. We suggest that newly designed$(Bu_4N)[Ru(DMFAdctpy)(NCS)_3]$ heteroleptic ruthenium complex would be a good candidate as a dye sensitizer of DSSCs, comparable to the N3.

Acknowledgment

This research was supported by the Basic Science Research Program through the National Research Foundation of Korea (NRF) funded by the Ministry of Education, Science and Technology (2010-0021668).

References

[1] Baldo, B., Regan, O. & Grätzel, M. (1991). *Nature (London)*., *353*, 737.

[2] Kuang, D., Ito, S., Wenger, B., Klein, C., Moser, J. E., Humphry-Baker, R., Zakeeruddin, S. M., & Grätzel, M. (2006). *J. Am. Chem. Soc*., *128*, 4146.; D. M. Chang, J. Y. Kim and Y. S. Kim. (2012). *Mol. Cryst. Liq. Cryst*., 567, 63.

[3] Kuang, D., Klein, C., Ito, S., Moser, J. E., Humphry-Baker, R., Zakeeruddin, S. M., & Grätzel, M. (2007). *Adv. Funct. Mater.*, *17*, 154.; D. M. Chang and Y. S. Kim. (2012). *J. Nanosci. Nanotechnol*., 12, 5709.

[4] Kuang, D., Klein, C., Ito, S., Moser, J. E., Humphry-Baker, R., Evans, N., Duriaux, F., Grätzel, C., Zakeeruddin, S. M., & Grätzel, M. (2007). *Adv. Mater.*, *19*, 1133.

[5] Nazeeruddin, M. K., Angelis, F. D., Fantacci, S., Selloni, A., Viscardi, G., Liska, P., Ito, S., Takeru, B. & Grätzel, M. (2005). *J. Am. Chem. Soc*., *127*, 16835.; D. M. Chang, J. Y. Kim and Y. S. Kim. (2012). *Journal of Korean Physical Society.*, in press.
[6] Wang, P., Klein, C., Humphry- Baker, R., Zakeeruddin, S. M., & Grätzel, M. (2005). *Appl. Phys. Lett*., *86*, 123508.
[7] Li, Jheng-Ying, Chen, Chia-Yuan, Chen, Jian-Ging, Tan, Chun-Jui, Lee, Kum-Mu, Wu, Shi-Jhang, Tung, Yung-Ling, Tsai, Hui-Hsu, Ho, Kuo-Chuan, & Wu, Chun-Guey, J. (2010). *Mater. Chem*., *20*, 7158.
[8] Horiuchi, T., Miura, H., Sumioka, K., & Uchida, S. (2004). *J. Am. Chem. Soc*., *126*, 12218.
[9] Tian, H., Yang, X., Cong, J., Chen, R., Liu, J., Hao, Y., Hagfeldt, A., & Sun, L. (2009). *Chem. Commun*., 6288.
[10] Haque, S. A., Handa, S., Peter, K, Palomares, E., Thelakkat, M., & Durrant, J. R. (2005). *Angew. Chem., Int. Ed*., *44*, 5740.
[11] Handa, S., Wietasch, H., Thelakkat, M., Durrant, J. R., & Haque, S. A. (2007). *Chem. Commun*., 1725.